Tetrahedron 66 (2010) 8267–8272

Contents lists available at ScienceDirect

Tetrahedron

journal homepage: www.elsevier.com/locate/tet

Mechanisms of the α,α-diphenylprolinol trimethylsilyl ether-catalyzed enantioselective aza-Michael reaction

Chiong Teck Wong *

*Institute of High Performance Computing (IHPC), Agency for Science, Technology and Research (A*STAR), 1 Fusionopolis Way, #16-16 Connexis, Singapore 138632, Singapore*

ARTICLE INFO

Article history:
Received 1 June 2010
Received in revised form 27 July 2010
Accepted 16 August 2010
Available online 21 August 2010

Keywords:
Ab initio calculation
Iminol intermediate
Enantioselectivity
Michael addition
Reaction mechanism

ABSTRACT

Depending on the nature of the aza-Michael donor, the C–N bond formation in the α,α-diphenylprolinol trimethylsilyl ether-catalyzed aza-Michael reactions was found to proceed via either (i) an iminol intermediate in a stepwise reaction, or (ii) a concerted reaction. This is contrary to the commonly proposed iminium mechanism for organocatalyst-catalyzed aza-Michael reactions. The iminol intermediate is formed from the reaction between the catalyst and the amine (Michael donor). These proposed mechanisms are able to account for the experimentally observed product enantioselectivity.

1. Introduction

The aza-Michael reaction[1] is a C–N bond-forming reaction between an α,β-unsaturated carbonyl compound (enal or enone) and an amine to afford a β-amino carbonyl compound. Recently, the group of Córdova has reported that the α,α-diphenylprolinol trimethylsilyl ether ((*S*)-**Cat1**) molecule catalyses the enantioselective aza-Michael reactions efficiently without the need for additives.[2–4]

The commonly proposed reaction mechanism for the (*S*)-**Cat1**-catalyzed aza-Michael reaction is that of the reaction proceeding via an iminium cation intermediate,[2–4] formed from the reaction between (*S*)-**Cat1** and an α,β-unsaturated carbonyl compound (Scheme 1). In the absence of (acid) additives, the first step of iminium formation would have to be a C–N bond formation between (*S*)-**Cat1** and an α,β-unsaturated carbonyl compound via a four-centre transition state. Our recent study on the (*S*)-**Cat1**-catalyzed α-functionalization of aldehydes with various nucleophiles revealed that the C–N bond formation step between (*S*)-**Cat1** and a carbonyl compound, via a four-centre transition state, is energetically unfavourable.[5] Furthermore, the possibility of OH^- (counter anion to the iminium cation) co-existing with the iminium cation in a non-polar solvent like $CHCl_3$ also seems unlikely. To better understand the function(s) of the (*S*)-**Cat1** catalyst, we report here our theoretical investigations on the mechanisms of the (*S*)-**Cat1**-catalyzed enantioselective aza-Michael reactions.

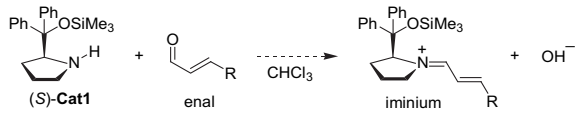

Scheme 1. Commonly proposed mechanism for the (*S*)-**Cat1**-catalyzed aza-Michael reaction, via an iminium intermediate.

2. Computational methods

Geometry optimizations were performed using the B3LYP hybrid density functional theory method[6] with the 6-31G* basis set for all molecular structures. All optimized geometries were verified to be equilibrium structures or transition states via frequency calculations. An equilibrium structure will have all real frequencies while a transition state will have one and only one imaginary frequency. The effect of solvent was studied using the polarization continuum model (PCM).[7] The solvation sphere size (ALPHA value) was set to 1.50 as this value is required to achieve optimization convergence for some transition states. The calculated energies were improved through $PCM_{solvent}$/MP2/6-311G** single-point energy solvation calculations. Unless otherwise noted, all energies (ΔE and $\Delta E^{\ddagger}$) reported are in kJ mol^{-1} and correspond to $PCM_{solvent}$/MP2/6-311G**//$PCM_{solvent}$/B3LYP/6-31G*, including $PCM_{solvent}$/B3LYP/6-31G* zero-point energy (scaled). A scaling factor of 0.9804[8] was used to correct for the directly computed $PCM_{solvent}$/B3LYP/6-31G*

* Tel.: +65 64191431; fax: +65 64632536; e-mail address: wongct@ihpc.a-star.edu.sg.

0040-4020/$ – see front matter © 2010 Elsevier Ltd. All rights reserved.
doi:10.1016/j.tet.2010.08.042

zero-point energies. All calculated enthalpy energies (ΔH and $\Delta H^{\ddagger}$) reported are in kJ mol^{-1} and correspond to PCM$_{solvent}$/B3LYP/6-31G* at the respective reaction temperature. All calculated Gibbs free energies (ΔG and $\Delta G^{\ddagger}$) reported are in kJ mol^{-1} and correspond to PCM$_{solvent}$/B3LYP/6-31G* at the respective reaction temperature. All calculations were performed using Gaussian 03.[9]

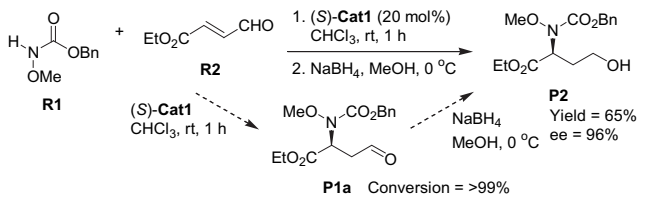

Scheme 2. (*S*)-**Cat1**-catalyzed aza-Michael reaction.[2]

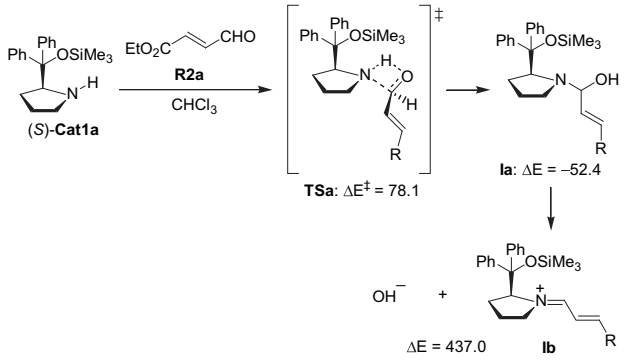

Scheme 3. C–N bond formation (**TSa**) between (*S*)-**Cat1a** and **R2a**, subsequently leading to the formation of iminium intermediate **Ib**. Calculated energy barrier ($\Delta E^{\ddagger}$) and reaction enthalpies (ΔE) correspond to the relative energy with respect to (*S*)-**Cat1a** (i.e., the free reactants), in kJ mol^{-1}.

3. Results and discussions

3.1. Aza-Michael reaction

The (*S*)-**Cat1**-catalyzed enantioselective aza-Michael reaction between *N*-methoxy amine-substituted ester (**R1**) and enal (**R2**) has been reported by Vesely et al.[2] (Scheme 2). For the reaction to proceed via an iminium mechanism, the first step would have to be

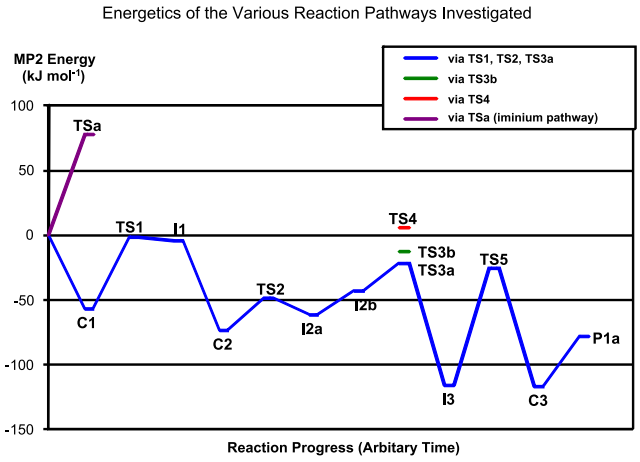

Figure 1. Calculated energy (MP2) profile of the iminol and iminium pathways.

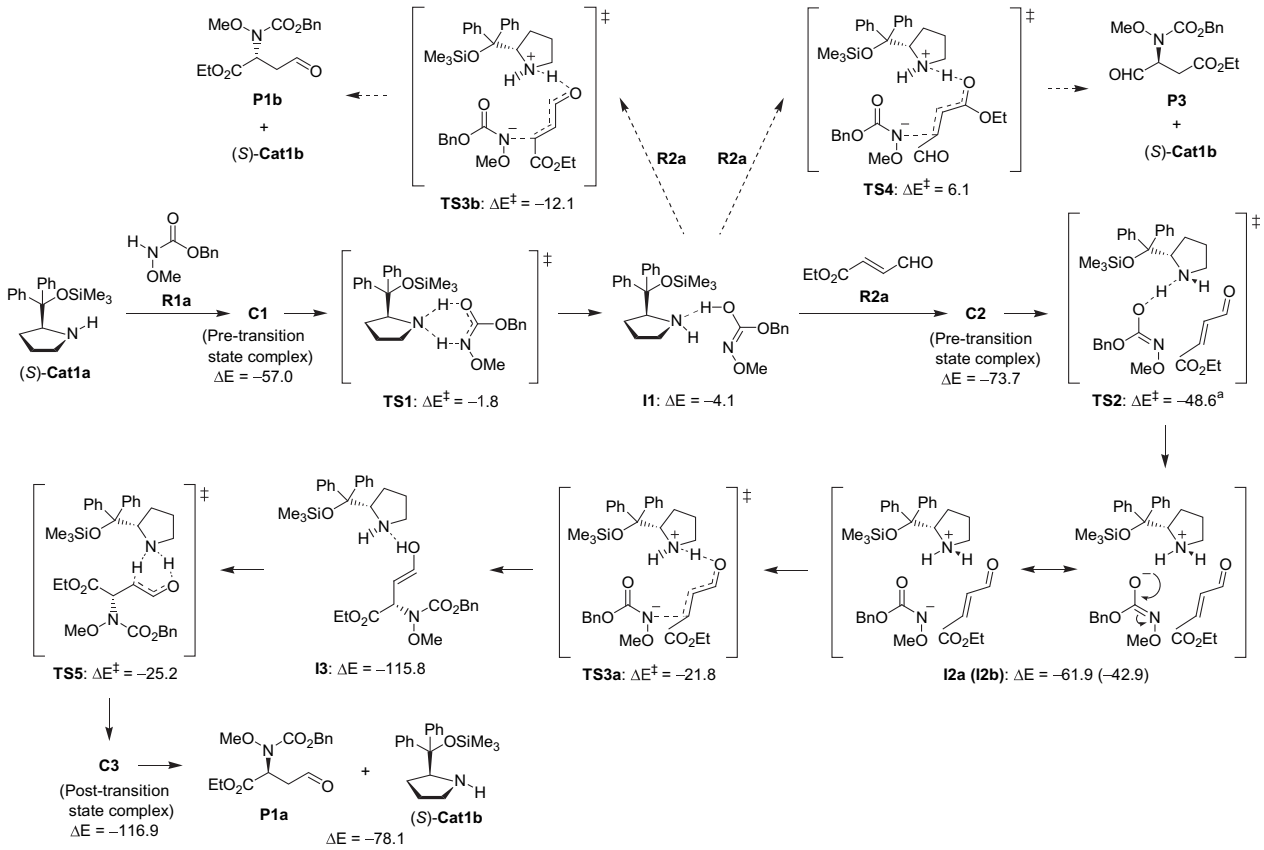

Scheme 4. Proposed reaction mechanism for the (*S*)-**Cat1**-catalyzed aza-Michael reaction, via an iminol intermediate. Calculated energy barriers ($\Delta E^{\ddagger}$) and reaction enthalpies (ΔE) correspond to the relative energy with respect to (*S*)-**Cat1a** (i.e., the free reactants), in kJ mol^{-1}. **I2a** and **I2b** are conformational isomers. [a]Estimated $\Delta E^{\ddagger}$ value from the difference between the calculated PCM$_{CHCl3}$/B3LYP/6-31G* electronic energy of **TS2** and **I2a**.

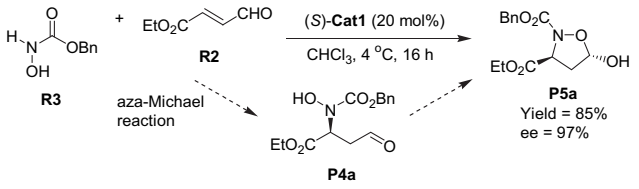

Scheme 5. (*S*)-**Cat1**-catalyzed aza-Michael/cyclization reaction.[3]

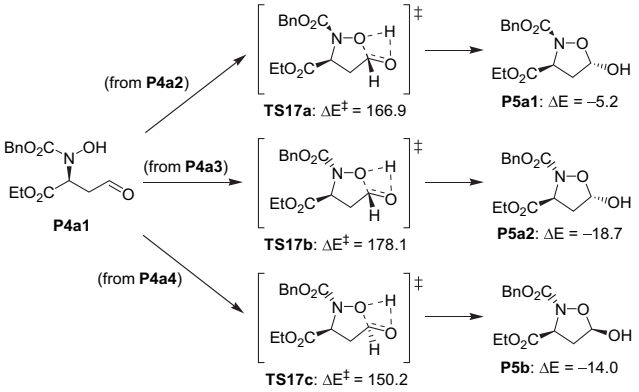

Scheme 6. Cyclization of **P4a**. Calculated energy barriers ($\Delta E^{\ddagger}$) and reaction enthalpies (ΔE) correspond to the relative energy with respect to **P4a1**, in kJ mol^{-1}. **P4a1**, **P4a2**, **P4a3** and **P4a4** are conformational isomers. **P5a1** and **P5a2** are conformational isomers.

a C–N bond-forming reaction between (*S*)-**Cat1a** and **R2a** via a four-membered cyclic transition state (**TSa**) (Scheme 3). Interestingly, the formation of the iminium cation (**Ib**) in $CHCl_3$ is calculated to be a highly endothermic process. This suggests that the (*S*)-**Cat1a**-catalyzed aza-Michael reactions do not proceed via an iminium intermediate.

A plausible reaction between (*S*)-**Cat1a** and **R1a** would be the tautomerization of **R1a** to an iminol via transition state **TS1** (Scheme 4). **TS1** corresponds to two simultaneous H-exchanges between (*S*)-**Cat1a** and **R1a** to form a (*Z*)-iminol-catalyst hydrogen-bonded complex (**I1**). The stereochemical orientation of **TS1** requires the amide's hydrogen and the carbonyl oxygen in **R1a** to be *syn* to each other, which effectively excludes the formation of the (*E*)-iminol.

The approach of the *Si* face of **R2a** towards **I1** results in the formation of intermediate **I2** via **TS2**. **TS2** consists of a H-shift from the O of the iminol to the N of (*S*)-**Cat1**. Next, a C–N bond formation occurs with a simultaneous H-shift from the N of (*S*)-**Cat1** to the O of **R2a** (**TS3a**) to form an enol-catalyst complex (**I3**). **I3** subsequently undergoes an enol–keto tautomerization reaction involving (*S*)-**Cat1** (via **TS5**) to afford the experimentally observed product **P1a**. Other plausible reaction pathways from **I3**, resulting in the formation of **P1a**, are calculated to be higher in energy (Scheme S3, in Supplementary data). Transitions states **TS3b** and **TS4**, which are analogous to **TS3a**, leading to possible products **P1b** (enantiomer of **P1a**) and **P3**, respectively, are calculated to be at least 9.7 kJ mol^{-1} higher in energy than **TS3a**. The proposed iminol

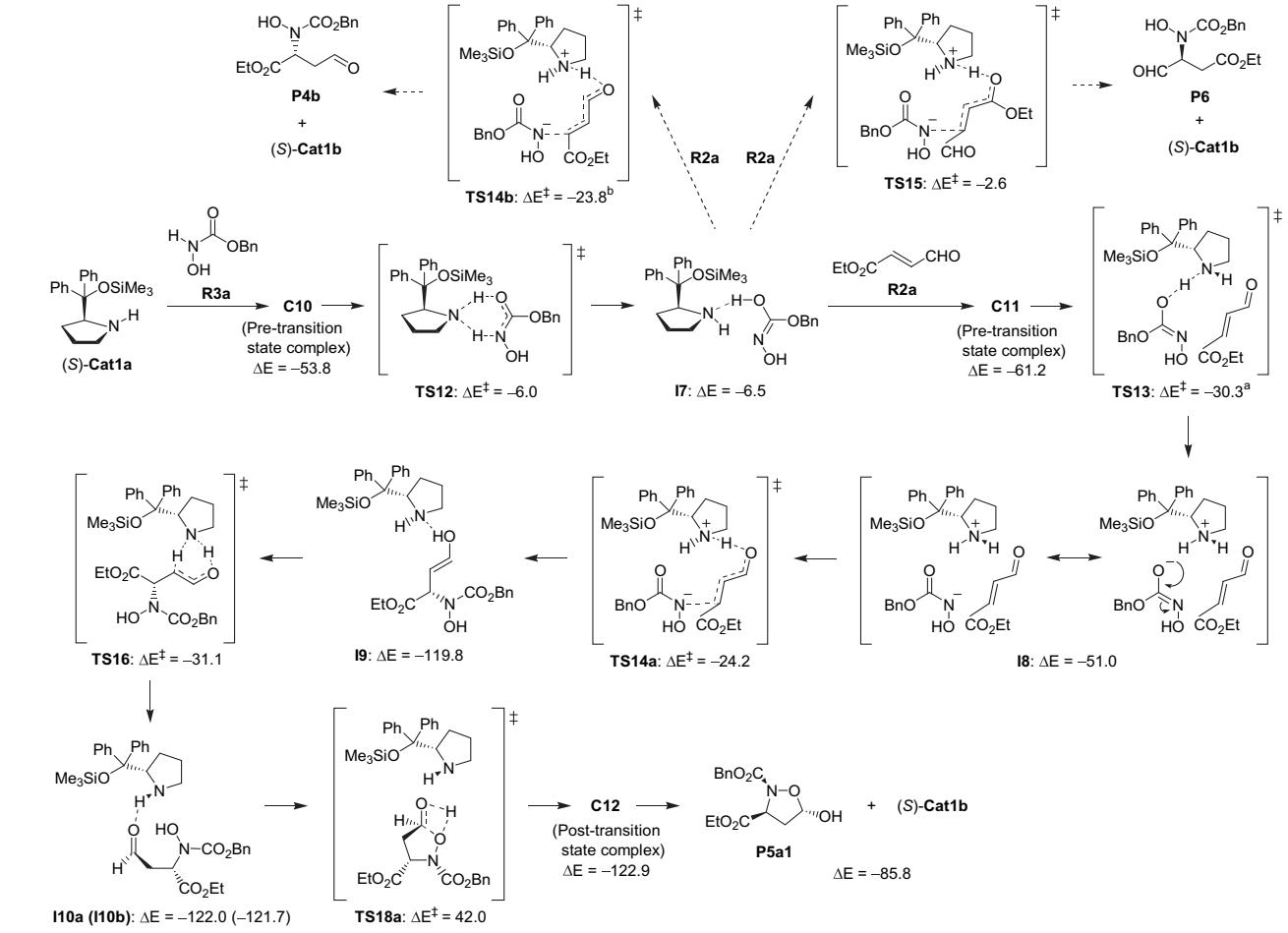

Scheme 7. Proposed reaction mechanism for the (*S*)-**Cat1**-catalyzed aza-Michael/cyclization reaction, via an iminol intermediate. Calculated energy barriers ($\Delta E^{\ddagger}$) and reaction enthalpies (ΔE) correspond to the relative energy with respect to (*S*)-**Cat1a** (i.e., the free reactants), in kJ mol^{-1}. **I10a** and **I10b** are conformational isomers. [a]Estimated $\Delta E^{\ddagger}$ value from the difference between the calculated PCM_{CHCl3}/B3LYP/6-31G* electronic energy of **TS13** and **I8**. [b]Estimated $\Delta E^{\ddagger}$ value from the difference between the calculated PCM_{CHCl3}/MP2/6-311G** electronic energy of **TS14a** and **TS14b**.

mechanism can fully account for the experimentally observed enantioselectivity and its calculated energy profile is lower in energy than the commonly proposed iminium pathway (Fig. 1). The calculated reaction enthalpy and Gibbs free energy profiles (Fig. S1, in Supplementary data) also show a similar profile.

In the above analysis of the iminol mechanism, we have considered the (*S*)-**Cat1a** conformation of the catalyst, where the H of the amine is pointing towards the $-C(Ph)_2(OSiMe_3)$ group. Conformational isomer (*S*)-**Cat1b**, where the H of the amine is pointing away from the $-C(Ph)_2(OSiMe_3)$ group (arising from the inversion of the lone pair of electrons on nitrogen) was found not to facilitate the iminol pathway (see Supplementary data for a discussion).

3.2. Aza-Michael/cyclization reaction

The (*S*)-**Cat1**-catalyzed enantioselective aza-Michael/cyclization reaction between *N*-hydroxy amine-substituted ester (**R3**) and enal (**R2**) has been reported by Ibrahem et al.[3] (Scheme 5). This reaction comprises of an aza-Michael reaction followed by a ring cyclization involving C–O bond formation. The expected product from the aza-Michael reaction is that of **P4a**. From **P4a1**, three transition states (**TS17a**, **TS17b** and **TS17c**) corresponding to the simultaneous C–O bond formation and 1,6-H shift, to afford **P5a** and **P5b** have been located (Scheme 6). Interestingly, the cyclization reaction from **P4a1** is predicted to yield primarily product isomer **P5b**, which is not in agreement with experimental observations. This suggests that the catalyst would have to play a role in controlling the stereochemistry during the cyclization reaction.

Following the iminol mechanism (Scheme 7), upon formation of the aza-Michael addition product-(*S*)-**Cat1** hydrogen-bonded intermediate (**I10a**), **I10a** undergoes conformation changes to that of **I10b**, from which the cyclization reaction takes place. The steric hindrance from the $-C(Ph)_2(OSiMe_3)$ group of (*S*)-**Cat1** dictates that the simultaneous C–O bond formation and 1,6-H shift (**TS18**) can only occur at the *Si* face of the aldehyde functional group, which affords the experimentally observed product isomer **P5a**. The calculated reaction energy profile is shown in Figure 2.

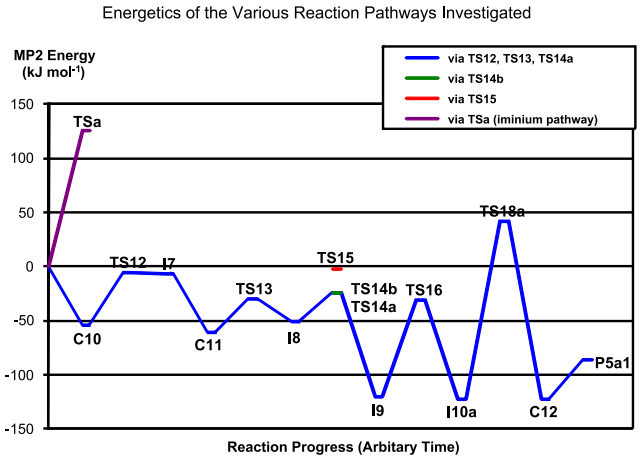

Figure 2. Calculated energy (MP2) profile of the iminol and iminium pathways.

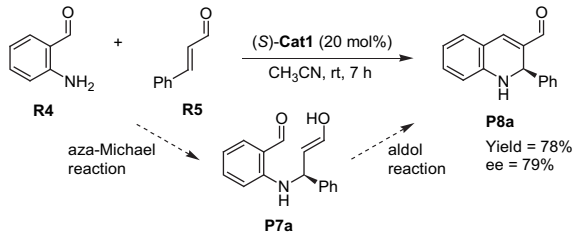

Scheme 8. (*S*)-**Cat1**-catalyzed aza-Michael/aldol reaction.[4]

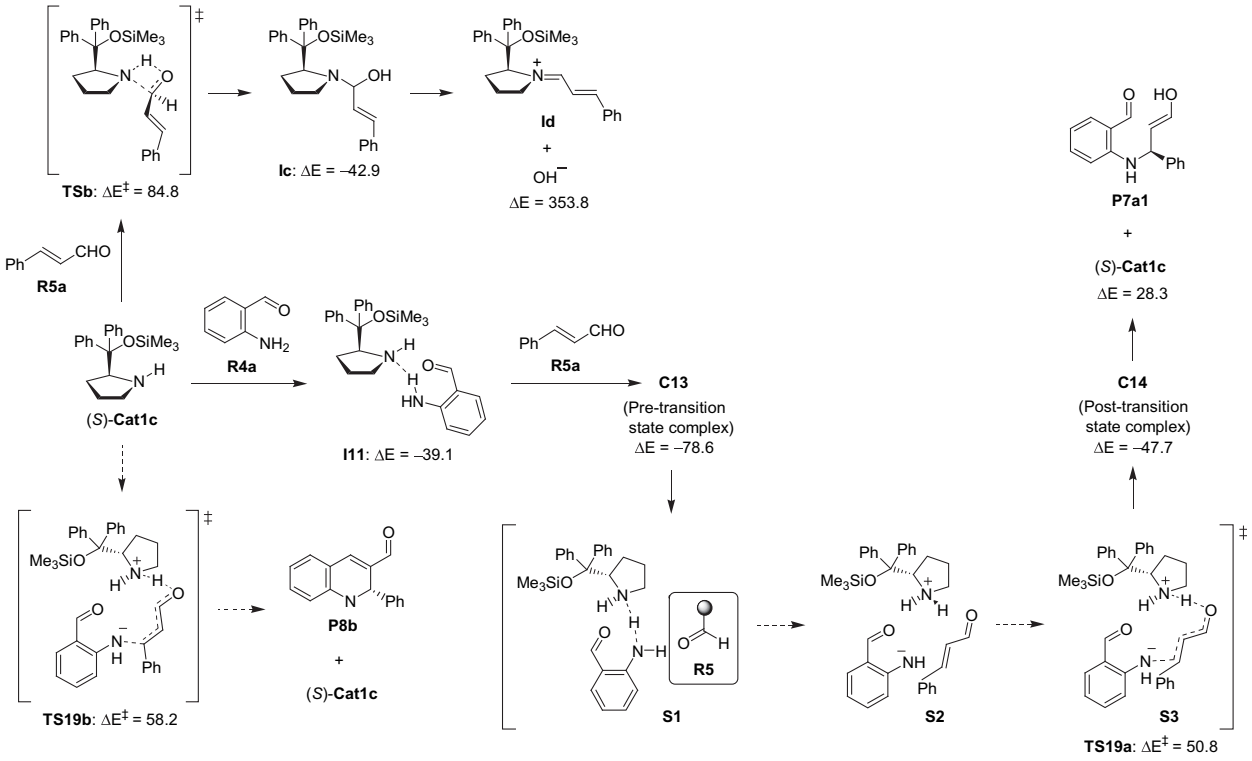

Scheme 9. Proposed reaction mechanism for the (*S*)-**Cat1**-catalyzed aza-Michael reaction between **R4** and **R5**. Calculated energy barriers ($\Delta E^{\ddagger}$) and reaction enthalpies (ΔE) correspond to the relative energy with respect to (*S*)-**Cat1c** (i.e., the free reactants), in kJ mol^{-1}.

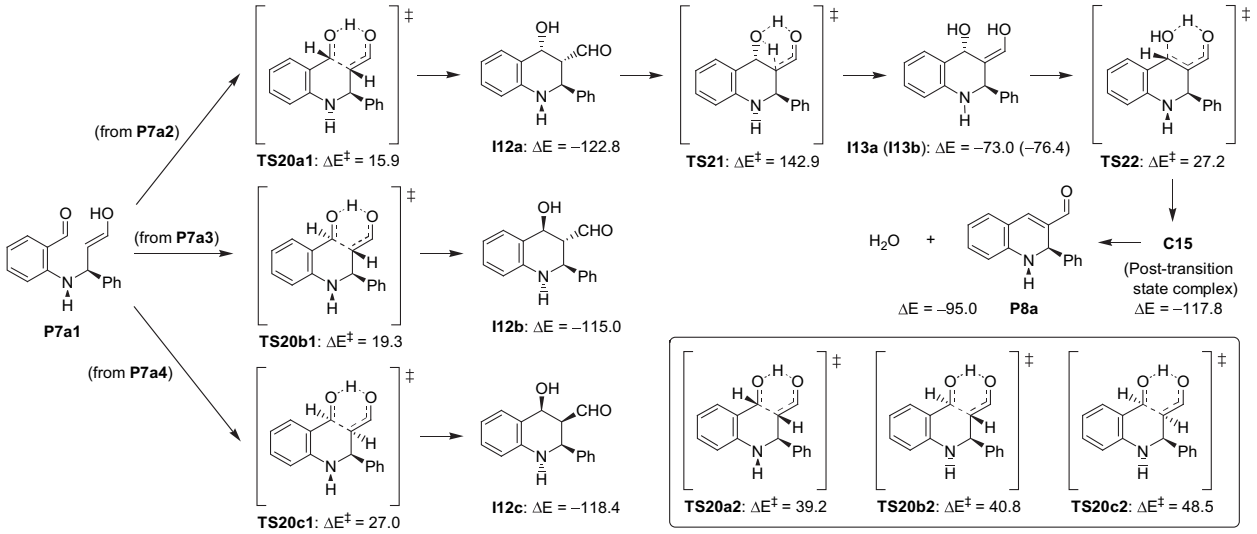

Scheme 10. Proposed reaction mechanism for the formation of **P8a** from **P7a**. Calculated energy barriers ($\Delta E^{\ddagger}$) and reaction enthalpies (ΔE) correspond to the relative energy with respect to **P7a1**, in kJ mol^{-1}. **P7a1**, **P7a2**, **P7a3** and **P7a4** are conformational isomers. **I13a** and **I13b** are conformational isomers.

3.3. Aza-Michael/aldol reaction

The (*S*)-**Cat1**-catalyzed enantioselective aza-Michael/aldol reaction between 2-aminobenzaldehyde (**R4**) and enal (**R5**) has been reported by Sundén et al.[4] (Scheme 8). This reaction involves first an aza-Michael reaction to form **P7a** followed by an intramolecular aldol reaction to afford **P8a**.

Interestingly, for this particular reaction, our calculations suggest that the aza-Michael reaction proceeds via a concerted transition state (**TS19a**) to form **P7a** (Scheme 9). **TS19a** is a late transition state depicting the simultaneous C–N bond formation and H-shift from the N of (*S*)-**Cat1c** to the O of **R5a** (structure **S3**). **TS19a** originates from complex **C13** and the prelude to transition state **TS19a** encompasses structures **S1** (a H-shift from the N of **R4a** to the N of (*S*)-**Cat1c**) and **S2**. The concerted nature of **TS19a** is confirmed with a combination of intrinsic reaction coordinate (IRC) calculations and optimization to a local minima procedure. No intermediate (ground state) structure corresponding to structure **S2** could be located. This interesting nature of **TS19a** is also observed when we switch to another theoretical method (DFT functional: PW91PW91).

Transition state **TS19b**, analogous to **TS19a**, which subsequently leads to product **P8b** (enantiomer of **P8a**) is calculated to be 7.4 kJ mol^{-1} higher in energy than **TS19a**.

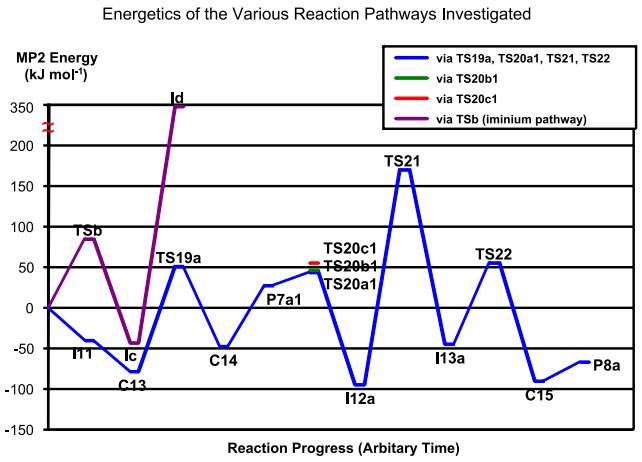

Figure 3. Calculated energy (MP2) profile of the (*S*)-**Cat1**-catalyzed aza-Michael/aldol reaction.

From **P7a**, an intramolecular aldol reaction occurs via **TS20a1** to afford **I12a** (Scheme 10). **I12a** subsequently undergoes a stepwise dehydration reaction (via **TS21** and **TS22**) to afford the experimentally observed product **P8a**. Transition states analogous to **TS20a1**, that lead to diastereomers **I12b** and **I12c**, are calculated to be at least 3.4 kJ mol^{-1} higher in energy than **TS20a1**. The calculated reaction energy profile is shown in Figure 3.

Investigations into the role of additives in the aza-Michael/aldol reaction suggest that additives catalyze the dehydration of **I12a** (see Supplementary data for a discussion).

4. Conclusion

The mechanism of the (*S*)-**Cat1**-catalyzed aza-Michael reactions was found to be dependent on the nature of the Michael donor (amine). The C–N bond formation in the (*S*)-**Cat1**-catalyzed aza-Michael reaction proceeds via either (i) an iminol intermediate in a stepwise reaction, or (ii) a concerted reaction. These proposed mechanisms are able to account for the experimentally observed product enantioselectivity and their calculated energy profiles are lower in energy than the commonly proposed iminium mechanism.

Acknowledgements

We thank Dr. Man-Fai Ng for helpful discussions.

Supplementary data

Conformational flexibility of intermediates and transition states, calculated Gibbs free energy barriers, directional approach of **R2a** towards **I1**, reactions involving (*S*)-**Cat1b** conformation, role of additives, Cartesian coordinates and absolute energies of all compounds. Supplementary data associated with this article can be found in the online version, at doi:10.1016/j.tet.2010.08.042.

References and notes

1. Enders, D.; Wang, C.; Liebich, J. X. *Chem.—Eur. J.* **2009**, *15*, 11058.
2. Vesely, J.; Ibrahem, I.; Rios, R.; Zhao, G.-L.; Xu, Y.; Córdova, A. *Tetrahedron Lett.* **2007**, *48*, 2193.
3. Ibrahem, I.; Rios, R.; Vesely, J.; Zhao, G.-L.; Córdova, A. *Chem. Commun.* **2007**, 849.
4. Sundén, H.; Rios, R.; Ibrahem, I.; Zhao, G.-L.; Eriksson, L.; Córdova, A. *Adv. Synth. Catal.* **2007**, *349*, 827.
5. Wong, C. T. *Tetrahedron* **2009**, *65*, 7491.

6. (a) Lee, C.; Yang, W.; Parr, R. G. *Phys. Rev. B* **1988**, *37*, 785; (b) Becke, A. D. *J. Chem. Phys.* **1993**, *98*, 5648.
7. (a) Cances, E.; Mennucci, B.; Tomasi, J. *J. Chem. Phys.* **1997**, *107*, 3032; (b) Mennucci, B.; Tomasi, J. *J. Chem. Phys.* **1997**, *106*, 5151; (c) Mennucci, B.; Cances, E.; Tomasi, J. *J. Phys. Chem. B* **1997**, *101*, 10506; (d) Cossi, M.; Barone, V.; Mennucci, B.; Tomasi, J. *Chem. Phys. Lett.* **1998**, *286*, 253; (e) Tomasi, J.; Mennucci, B.; Cances, E. *J. Mol. Struct. (Theochem)* **1999**, *464*, 211; (f) Cossi, M.; Scalmani, G.; Rega, N.; Barone, V. *J. Chem. Phys.* **2002**, *117*, 43.
8. Wong, M. W. *Chem. Phys. Lett.* **1996**, *256*, 391.
9. Frisch, M. J.; Trucks, G. W.; Schlegel, H. B.; Scuseria, G. E.; Robb, M. A.; Cheeseman, J. R.; Montgomery, J. A., Jr.; Vreven, T.; Kudin, K. N.; Burant, J. C.; Millam, J. M.; Iyengar, S. S.; Tomasi, J.; Barone, V.; Mennucci, B.; Cossi, M.; Scalmani, G.; Rega, N.; Petersson, G. A.; Nakatsuji, H.; Hada, M.; Ehara, M.; Toyota, K.; Fukuda, R.; Hasegawa, J.; Ishida, M.; Nakajima, T.; Honda, Y.; Kitao, O.; Nakai, H.; Klene, M.; Li, X.; Knox, J. E.; Hratchian, H. P.; Cross, J. B.; Adamo, C.; Jaramillo, J.; Gomperts, R.; Stratmann, R. E.; Yazyev, O.; Austin, A. J.; Cammi, R.; Pomelli, C.; Ochterski, J. W.; Ayala, P. Y.; Morokuma, K.; Voth, G. A.; Salvador, P.; Dannenberg, J. J.; Zakrzewski, V. G.; Dapprich, S.; Daniels, A. D.; Strain, M. C.; Farkas, O.; Malick, D. K.; Rabuck, A. D.; Raghavachari, K.; Foresman, J. B.; Ortiz, J. V.; Cui, Q.; Baboul, A. G.; Clifford, S.; Cioslowski, J.; Stefanov, B. B.; Liu, G.; Liashenko, A.; Piskorz, P.; Komaromi, I.; Martin, R. L.; Fox, D. J.; Keith, T.; Al-Laham, M. A.; Peng, C. Y.; Nanayakkara, A.; Challacombe, M.; Gill, P. M. W.; Johnson, B.; Chen, W.; Wong, M. W.; Gonzalez, C.; Pople, J. A. *Gaussian 03, Revision C.01*; Gaussian: Wallingford, CT, 2004.